Results in Chemistry 14 (2025) 102096

Contents lists available at ScienceDirect

Results in Chemistry

journal homepage: www.sciencedirect.com/journal/results-in-chemistry

# Phytic acid modified polycaprolactone electrospun matrix for active nerve regeneration

Ganesh Prasad Awasthi [a,1], Arjun Prasad Tiwari [b,1], Miyeon Shin [c], Krishna Prasad Sharma [a], In Hong Yang [b,*], Changho Yu [a,c,**]

[a] Division of Convergence Technology Engineering, Jeonbuk National University, Jeonju, Jeollabuk-do, 54896, Republic of Korea
[b] Center for Biomedical Engineering and Science, Department of Mechanical Engineering and Engineering Science, University of North Carolina at Charlotte, Charlotte, North Carolina 28223, United States
[c] Department of Energy Storage/Conversion Engineering of Graduate School (BK21 FOUR), Jeonbuk National University, Jeonju, Jeollabuk-do, 54896, Republic of Korea

ARTICLE INFO

*Keywords:*
Phytic acid
Polycaprolactone
Electrospinning
DRG neurons

ABSTRACT

Physicochemical modification of biomaterials has enormous potential for enhanced functionality and applications. Phytic acid (PA) is a sustainable, non-toxic, and environmentally friendly material used for surface modification in different applications. However, the impact of PA on the surface of the biomaterial matrix and its response to nerve cells has not been studied as far as we know. In this study, we fabricated PA-embedded polycaprolactone (PCL) nanofibrous scaffolds using the electrospinning method and studied the potentiality of these scaffolds for primary sensory neuron growth and alignment. The nanofiber morphology of the scaffolds was evaluated using field emission electron microscopy (FESEM). The results showed that the fiber orientation and diameter were dependent on the amount of PA in the electrospinning solution. The degree of orientation of the aligned nanofibers was higher than that of their random counterparts in composite scaffolds. The PA-loaded nanofibers were found to have higher compatibility with dorsal root ganglia (DRG) neuron cells than the corresponding fibers without PA. Further, the PA provided guidance for axon growth along the matrix. Overall, the results suggested that embedding PA into the scaffold could be a better approach for enhancing nerve growth and alignment, which is required for nerve regeneration.

## 1. Introduction

The incidence of peripheral nerve injury is growing in the aged population owing to increased road and industrial accidents and severed disease states [1,2]. The recovery rate of conventional autograft models is often inadequate when addressing large gaps. In this context, the process of tissue repair depends on a thorough understanding of how the microenvironment regulates cellular behavior [3]. Biomaterials have gained increasing interest in facilitating nerve injury repair and are often used in tissue regeneration. They are composed of natural and synthetic polymers [4–6]. Generally, sets of designed biomaterials, such as hydrogels, nanofibers, sponges, biomaterial ink, and 3D/4D constructs, have been of great interest over the last decade [7–10]. The challenge of regenerating nerve tissue has been addressed using Poly-L-lactide (PLLA), polycaprolactone (PCL), polyglycolic acid (PGA) nanofibers *in vitro* and in animal models [11,12]. However, the polymeric biomaterial itself may not be enough to regenerate tissues, including neurons, due to its functionality and bioactivity. Mimicking physiological resemblance and increasing bioactivity are good approaches for achieving tissue regeneration.

Many reports have demonstrated the improved nerve regeneration capability of polymeric nanofibers synthesized by electrospinning [13,14]. Electrospun nanofibers have been reported to have many advantageous properties, including structural resemblance to the extracellular matrix and the possibility of tuning mechanical, wettability, and biological properties for tissue growth [15–18]. In addition, electrospun nanofibers work well as drug delivery vehicles because they can hold a variety of medications, growth factors, and other bioactive substances to impart biological cues and functions to the scaffolds in the produced state [19]. The prerequisite criteria for achieving enhanced regeneration

* Corresponding author.
** Corresponding author at: Division of Convergence Technology Engineering, Jeonbuk National University, Jeonju, Jeollabuk-do, 54896, Republic of Korea.
*E-mail addresses:* iyang3@charlotte.edu (I.H. Yang), goody0418@jbnu.ac.kr (C. Yu).
[1] Equally contributed.

https://doi.org/10.1016/j.rechem.2025.102096
Received 28 November 2024; Accepted 2 February 2025
Available online 4 February 2025

by scaffolding materials is that they should possess bioactivity along with the physiological properties.

Bioactive compounds can be encapsulated into electrospun nanofibrous scaffolds for tissue regeneration [20]. Similarly, physical modification of the matrix in terms of morphology and orientation can enhance nerve cell growth [21]. Several studies have shown that the addition of hydrophilic bioactive chemicals improves the mechanical characteristics, degradation rate, hydrophilicity, and *in vivo* shrinkage of PCL scaffolds. The regulated electrospinning and solution parameters may influence these physical characteristics [22,23].

The gadget may create random or aligned fibers based on three main parameters: voltage, flow rate, and working distance [23,24]. The encapsulation of growth factors and drug compounds and the control of their release into the milieu enhanced the suitability of the fibrous matrix. However, the encapsulation of the growth factors faces many challenges owing to their delicate structure and the harsh electrospinning process under high voltage. High immunogenicity has also been reported in real-world settings [25]. There has been a growing interest in identifying compounds that enhance the regeneration process and repair mechanism [26]. In this context, this study aimed to propose PA, a naturally occurring compound with anti-inflammatory and antioxidant properties that can enhance peripheral nerve growth and improve regeneration by controlled and sustained release from a polymeric substrate. Phytic acid, mostly found in cereals, milk, nuts, and grains, has been stated to have several health benefits under normal and diseased conditions [27,28]. PA protects neurons from Alzheimer's disease [29] and chemotherapeutics induced peripheral neuropathy [27]. More commonly, it has been used as a crosslinker to create hydrogel networks because of its abundance of chelating functional groups [30]. Our recent study showed that PA maintains peripheral neuron integrity and enhances survivability [27]. To the best of our knowledge, the perspective on the nerve regeneration capability of electrospun nanofibers with PA has not yet been reported.

PCL is a synthetic polymer, and its electrospun nanofibrous scaffolds have been widely used in tissue regeneration because of their non-toxicity, tunable mechanical properties, good electrospinning properties, ability to achieve high material purity, and slow degradation profile [31–33]. Numerous studies including ours have shown that PCL scaffolds support the cell adhesion, proliferation, and differentiation. However, the low wettability and degradability of this polymer presents a major drawback. [31,34,35]. Herein, we encapsulated of PA into the PCL nanofibrous scaffolds to improve peripheral neuronal cell growth by improving the hydrophilicity of the PCL nanofiber. The result demonstrates that the PA concentration in the electrospun nanofibers altered the morphology of the PCL scaffolds. The PA contained PCL scaffolds had significantly reduced fiber diameters compared with pristine PCL scaffolds. Besides, PCL/PA0.5 scaffold have shown neural cell growth and alignment.

## 2. Materials and methods

Polycaprolactone (PCL; $M_W$ = 80,000 g/mol), and 2,2,2-Trifluoroethanol (TFE) were purchased from Sigma-Aldrich, USA; Phytic acid (PA) solution ($C_6H_{18}O_{24}P_6$) was purchased from Shanghai Aladdin Biochemical Technology Co., Ltd. All analytical grade materials were used without any additional purification.

### 2.1. Preparation of electrospinning solutions

PCL pellets (2 g) were dissolved in 19.5 g of TFE by magnetic stirring overnight. Then, different amounts (0.5 and 2 g) of phytic acid solution were slowly added to the PCL solutions under stirring and continued overnight at room temperature. In addition, only the PCL solution was prepared without PA.

### 2.2. Fabrication of PCL/PA nanofibrous scaffolds

The 12 mL plastic syringe with a metal nozzle (23-gauge, 0.26 mm diameter) was filled with all the prepared solutions. The following parameters were used in the NanoNC electrospinning system: Solution flow rate: 1 mL/h; applied voltage, 17 kV; nozzle tip to collector distance, 100 mm; and collector drum speed, ~ 2000 rpm. Electrospinning was performed at ambient temperature. The nanofibers prepared by adding PA 0.5 mL and 2 mL to the PCL solution were denoted PCL/PA0.5 and PCL/PA2, respectively.

### 2.3. Characterization of scaffolds

Field-emission scanning electron microscopy (FESEM, Carl Zeiss, supra 40 VP, Japan) was used to examine the surface morphology of the nanofibrous scaffolds. The crystallographic structures of the materials were analyzed using an X-ray diffractometer (XRD; Rigaku, Japan) with Cu Kα (= 1.540 Å) radiation over Bragg angles ranging from 10 to 50°. Functional group were studied using Fourier transform infrared spectroscopy (FTIR; Perkin Elmer, USA). Thermal degradation analysis with thermogravimetric analysis (TGA) and differential scanning calorimetry (DSC) were conducted under a $N_2$ atmosphere from room temperature to 800 °C at a heating rate of 10 °C/min using TA instruments, SDT650. The water contact angle of PCL and PCL/PA0.5 scaffolds were measured using SEO Phoenix 300 Touch, with 1 μL drop volume.

### 2.4. Dorsal root ganglia (DRG) neurons extraction and culture

All animal experiments were performed in accordance with the procedures authorized by the University of North Carolina Charlotte's Institutional Animal Care and Use Committee (IACUC 20–013). DRG neurons were obtained from the embryos of an E15 pregnant Sprague Dawley rat under a flow of isoflurane (7.5 L/min). The embryos were dissected using a stereoscopic dissection microscope (Nikon SMZ745T, Japan). DRG cells were collected by dissecting the spinal column and were later dissociated as previously reported [27]. Briefly, 2 mL of DRG clumps comprising L15-P/S media was incubated with 1 mL of collagenase (10 mg/mL in L15-P/S) and 1 mL of DNAse (0.5 mg/mL) for 30 min, after which it was subjected to centrifugation. The cells were further treated to 0.25 % trypsin for 5 min at 37 °C, neutralized with fresh medium containing FBS, and centrifuged to collect the DRG cells. The cells were then re-suspended in a DRG culture medium at a concentration of 100,000 cells/mL and seeded on the 96-wells (200 μL) unless otherwise stated. The DRG culture medium consisted of neurobasal medium supplemented with 1 % 100× P/S, 1 % glucose, 100 × 2 % glutamate, 2 % B27 supplement, and 20 ng/mL nerve growth factor (NGF). 5-Fluoro-2′-deoxyuridine (FUdR) (13 μg/mL) was added to the culture medium to exclude possible non-neuronal glial cells. The cell culture was maintained by replenishing the half-well media every 72 h.

### 2.5. Axon lengths measurement and neuronal alignment

Various PA loaded nanofiber scaffolds of 1 $cm^2$ were attached to the 6 well Petri dishes using medical grade adhesive and sterilized by the UV light exposure for 2 h in a cell culture hood.

The effect of PA on neurons were studied in terms of changes in axon length. One thousand DRG cells in the cell culture suspension were seeded onto culture plates containing nanofibrous sample. After 48 h of culture the cells were stained with 5 μM Calcein-AM dye (Corning, USA) containing media followed by live-cell images by fluorescence microscope (Leica DM i8, Germany). Image J software (Java 1.8.0_345 (64-bit)) was used to estimate the axon length. At least 50 axons were selected from triplicate samples to calculate the average axon length.

### 2.6. Statistical analysis

All data were presented as a mean ± standard error (SE) ($n = 3$). The probability value ($P$-value) between groups was analyzed using one-way analysis of variance (ANOVA) followed by Tukey's post-hoc test for multiple comparisons. Statistical significance was set than 0.05 significant.

## 3. Results and discussion

The morphologies and fiber diameter distributions of the as synthesized electrospun nanofibrous scaffolds were evaluated using FESEM and ImageJ software, respectively. The FESEM images showed that the PCL/PA0.5 and PCL nanofibers were almost aligned in the micrographs at low and high magnifications. As the amount of PA in PCL solution increased, the fiber dimeter in the scaffolds decreased. Correspondingly, the diameters of PCL, PCL/PA0.5, and PCL/PA2 fibers were 983 ± 266 nm, 268 ± 186 nm and 95 ± 192 nm, respectively. The reduced fiber diameter of PCL/PA2 was nineteen-fold less than that of the pristine PCL NFs scaffold. In addition, it was found that the PCL/PA2 had more randomness in the nanofibers than the PCL and PCL/PA0.5 scaffolds. The elemental mapping, EDS spectrum, and quantification of PCL/PA0.5 and PCL/PA2 NFs are depicted in Fig. 1(g, h) respectively. The results show that the C, O, and P were noticeable. Moreover, an increase the amount of Phosphorous Wt% is consistent with the increasing amount of PA concentration in the electrospinning solution.

The XRD patterns of pristine PCL and PCL/PA are presented in Fig. 2 (a). The sharp diffraction peaks are clearly depicted at $2\theta = 21.3°$ and 23.7° corresponding to the crystal plane of (110) and (200) in PCL scaffolds. While PA containing PCL, scaffolds showed lower crystalline peaks at the same angle of 2θ. The result indicated that PA incorporation into the PCL nanofibrous scaffolds reduced the crystallinity, as indicated by the lower intensity peaks of the PCL/PA samples [36,37].

FTIR spectra of the PCL and PCL/PA nanofibrous scaffolds are shown

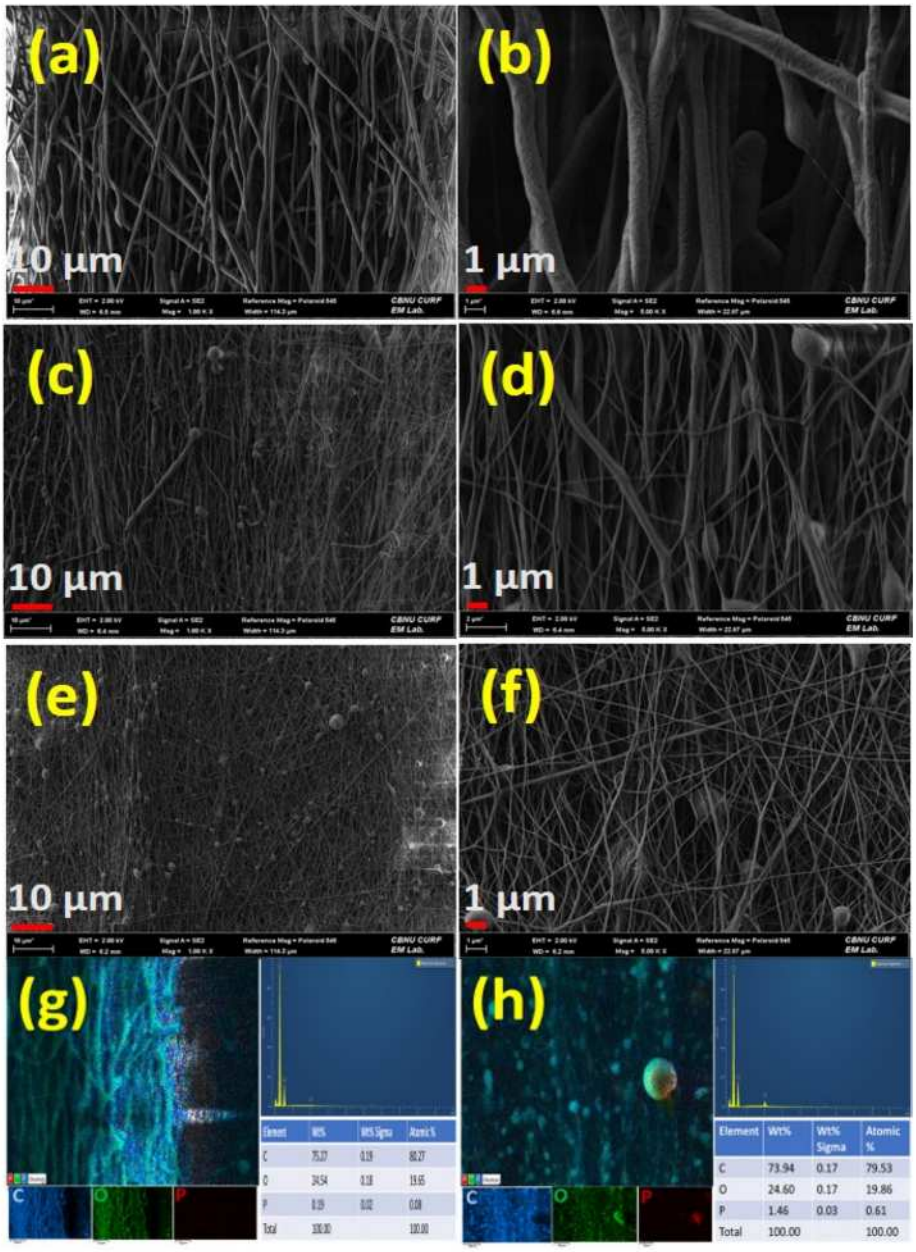


**Fig. 1.** FESEM images of (a, b) pristine PCL; (c, d) PCL/PA0.5; (e, f) PCL/PA2 NFs scaffolds with low and high magnification respectively. (g, h) color mapping with the EDX spectra of PCL/PA0.5 and PCL/PA2 NFs, respectively.

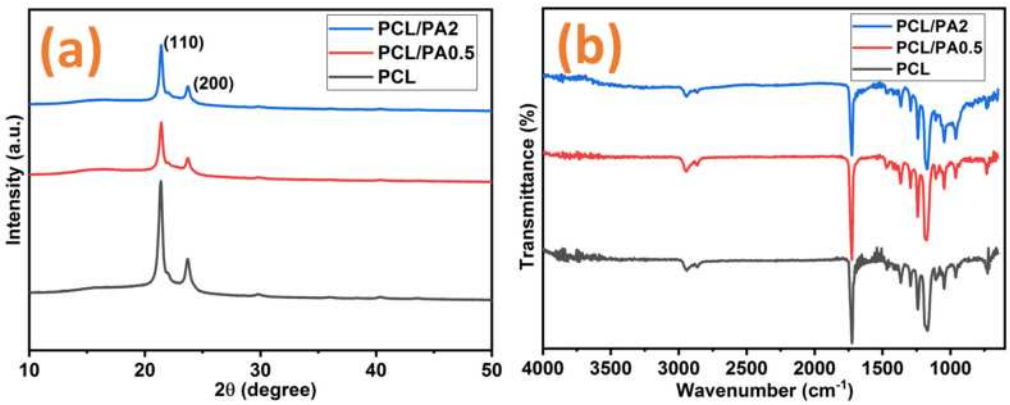


**Fig. 2.** (a) XRD and (b) FTIR of PCL, PCL/PA0.5, and PCL/PA2 NFs.

in Fig. 2(b). For the pristine PCL, it can be seen that the characteristic bands of 2949.83 $cm^{-1}$ (C—H asymmetric stretching vibration), 2866.66 $cm^{-1}$ (C—H symmetric stretching vibration), 1729.10 $cm^{-1}$ (C═O stretching), 1469.73 $cm^{-1}$ and 1365.42 $cm^{-1}$ (C—H scissoring and symmetric deformation), 1293.53 $cm^{-1}$ (C—O and C—C stretching), 1246.31 $cm^{-1}$ (C-O-C asymmetric stretching vibration), 1170.89 $cm^{-1}$ (O-C-O stretching vibration), 1113.10 $cm^{-1}$ (C—O stretching), 1047.21 $cm^{-1}$ (C—O stretching) are existed [38]. In addition, the peak existed at 1047.21 $cm^{-1}$ sifted towards 1045 $cm^{-1}$ and the intense peak exhibited at 668.17 $cm^{-1}$ (P—O) in PA/PCL scaffolds. The peak existed at 1005 $cm^{-1}$ belongs to the phosphate group [39].

The thermal behaviors of the synthesized nanofibers are shown in Fig. 3. The TGA (Fig. 3(a)) result showed that PCL/PA2 nanofibers have two weight loss stages (*i.e.*, moisture evaporation and thermal degradation) at about 100 °C and 350 °C, respectively [40]. While, pristine PCL and PCL/PA0.5 have a slower degradation rate as compared to PCL/PA2 nanofibers, Though, a lower weight loss or a higher residual weight percentage of PCL/PA2 was obtained after the thermal degradation stage, The fast decomposition of PCL/PA2 in moisture evaporation and thermal decomposition might be due to the beads that exist in nanofibers. The PCL, PCL/PA0.5, and PCL/PA2 contained 2.49 %, 3.05 %, and 4.28 % residual weight, respectively. Furthermore, the crystal melting behavior of the samples was studied using DSC analysis (Fig. 3 (b)). The DSC thermogram of the PCL shows a broad melting peak at about ~70 °C. The PA- incorporated samples showed a remarkable melting peak shift compared with that of PCL. The mild peak shifts towards lower temperature (~ 65 °C) for PCL/PA0.5, while peak shifts towards upper temperature (~72 °C) for the sample PCL/PA2. The results showed that the hydrophilic nature of PA had changed the melting behavior of PCL in PCL/PA composite nanofibers [41]. (See Figs. 4 and 5.)

Phytic acid, in the form of P, is a biological molecule that plays a crucial role in energy storage. Similarly, inositol, a derivative of phytic acid, is involved in various signaling pathways that regulate cellular processes such as growth, survival, and differentiation [42]. However, its positive effects on health have been underestimated by misinterpreted as an antinutrient compound. Calcium, magnesium, and zinc are vital elements for cellular activities. It has been assumed that the binding of these elements to phytic acid results in low bioavailability at the cellular level and subsequent negative consequences for cellular activities. To observe the effects of phytic acid on biomaterial scaffolds, we cultured dorsal root ganglion cells on nanofibers with different concentration of PA. The results clearly show that all nanofibers supported the extension of the DRGs along the nanofiber orientation. However, the PCL/PA0.5 fibers have shown increased axonal networks compared to pure PCL and PCL/PA2 fibers. Interestingly the cells on the glass discs had no specific axon orientation and had shorter axons than the cells on the nanofiber substrates ($P > 0.05$).

The increased axons length of PA-containing fibers compared with that of non-PA-containing fibers suggests that PA plays a key role in axon growth. However, increasing the PA concentration in the fibers resulted in slightly shorted axons growth, indicating that the PCL/PA0.5 fiber substrate can be a choice among others to achieve neurogenesis. The nervous system contains relatively higher concentration of PA up to 5.5 mM.

These nanofibers mimic the extracellular matrix, with which collagen fibers are largely associated. Therefore, nanofibers support the initial cell attachment, growth, and migration [43]. Numerous studies have shown that nanofibers support neurogenesis. However, cells activities are limited to synthetic nanofibers owing to bio-functional deficiencies. A previous report showed that cells adhered well during the first 2 h and extended to form cellular network on the nanofibrous substrate with albumin functionalization compared to non-functionalized nanofibers [44]. Biomolecules are widely encapsulated

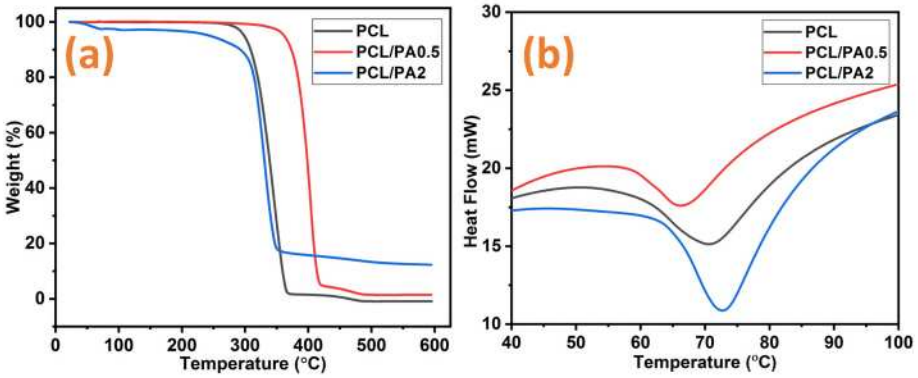


**Fig. 3.** (a) TGA and (b) DSC of PCL, PCL/PA0.5, and PCL/PA2 NFs.

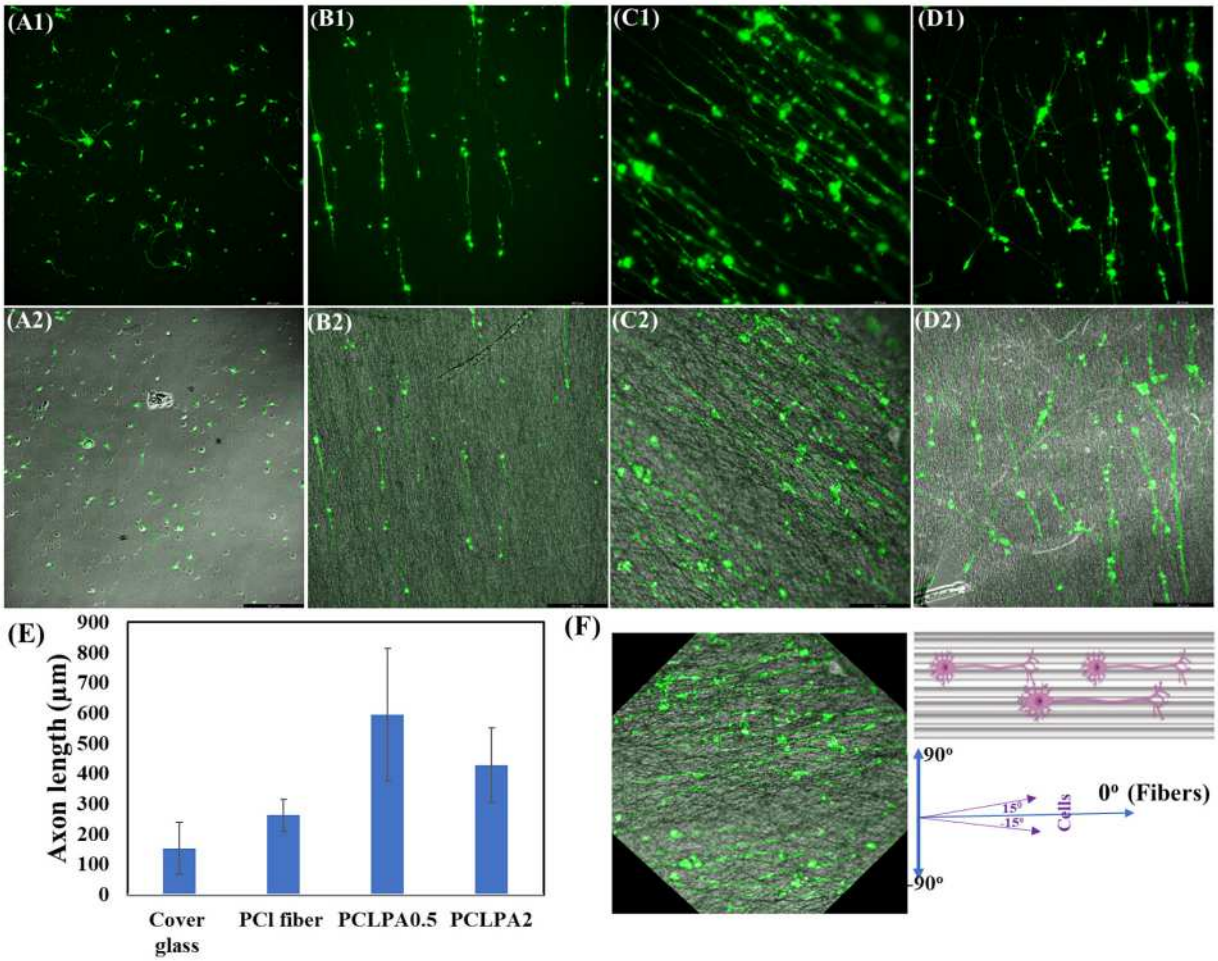


**Fig. 4.** DRGs growth on the nanofiber substrates. DRGs on glass substrate (A1, A2), pristine PCL (B1, B2), PCL/PA0.5 (C1, C2), and PCL/PA2 (D1, D2). 1 and 2 correspond to the florescence images and merged images, respectively. Axon length on different substrates (E) and alignment of the DRGs growth on the PCL/PA0.5 fiber substrate (F). The nanofiber orientation is considered as 0° and angle of axons on nanofibers was measured using Image J. ** represent $P < 0.01$ and *** represents $P < 0.001$.

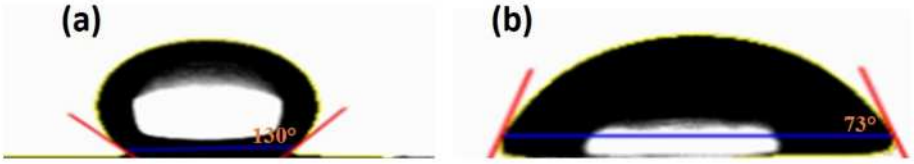


**Fig. 5.** Average water contact angles of: (a) PCL nanofibers, and (b) PCL/PA0.5 respectively.

in the regenerative substrates to enhanced cellular growth, tissue repair, and rapid recovery.

Peripheral nerves are well-extended network distally from the median body; therefore, they are more susceptible to getting injured by injuries, accidents, aging populations, and diseased condition. Thus, a substrate with a high potential for nerve regeneration is anticipated. Modulation of nerve cells by maintaining the substrate architecture and functionalization is a well-versed strategy. Phytic acid is commonly used as a crosslinker to make substrates more likely than as a functional molecule to enhance cell growth and regeneration. We first loaded PA into the nanofiber matrix and evaluated its effect on DRGs neurons as a peripheral neuron. Substrates are often coated with poly-D-lysine and laminin prior to primary DRGs culture. Interestingly, the PA-loaded nanofibers exhibit remarkable growth along the axis. The nanofibers in the 0.5 PA fibers allow the axons growth almost along the fiber axis. The enhanced alignment of axons was attributed to the aligned fibrous structure. Another reason for the enhanced axonal growth in the PA-containing fibers may the increased wettability of the fibers.

PCL has a hydrophobic surface (average contact angle of ~130°), with which cells initially tend to exhibit low adhesion. In contrast the PCL/PA0.5 fibers were ~ 73° which is hydrophilic, supporting neuronal attachment and growth over the axis of the nanofiber. The increased wettability of PCL/PA nanofibers can enhance the degradation rate by introducing hydrophilic sites ($PO_4^{3-}$ and -OH groups) of the PA [45,46], which promote PCL hydrolysis. Interestingly PCL/PA0.5 fibers had lower axon lengths. This suggests that the burst release of PA at this level may not support cellular processes. Since the cells underwent vigorous steps prior to seeding, they may not initially be tolerant to higher concentrations of PA in the release medium. PCL/PA electrospun NFs have shown promise in nerve regeneration due to their ability to mimic the extracellular matrix and provide a supportive scaffold for cell growth. However, they may have some limitations.

"While generally considered biocompatible and bioactive, phytic acid's concentration must be carefully controlled to avoid cytotoxic effects, particularly at higher levels [27]. Similarly, the dense structure of electrospun sheets can limit cell infiltration and migration into the scaffold [47], which may hinder tissue integration and the formation of functional neural networks. To address these limitations, we have considered developing porous and three-dimensional hierarchical nanofibrous scaffolds that facilitate efficient nutrient and oxygen diffusion while promoting the formation of three-dimensional neural networks in future works".

## 4. Conclusions

Phytic-acid-loaded PCL nanofiber scaffolds were successfully synthesized by the electrospinning method. The nerve regenerative effect of PA on PCL nanofibrous scaffolds was evaluated using DRG neural cells *in vitro*. The topography and physicochemical characteristics of the scaffolds revealed the significant impact of PA on the PCL nanofibers. The results showed that PA-embedded PCL scaffolds had reduced fiber diameters, low crystallinity, improved hydrophilicity, and good thermal stability compared with pristine PCL. Besides, the PCL/PA0.5 scaffold provided a promising ECM for DRG neural cell growth and alignment. Overall, the results highlight that PA-modified nanofibers can be promising biomaterials for nerve regeneration.

## CRediT authorship contribution statement

**Ganesh Prasad Awasthi:** Writing – review & editing, Writing – original draft, Validation, Methodology, Investigation, Formal analysis, Data curation, Conceptualization. **Arjun Prasad Tiwari:** Writing – review & editing, Writing – original draft, Validation, Methodology, Investigation, Formal analysis, Data curation, Conceptualization. **Miyeon Shin:** Validation, Methodology, Investigation, Formal analysis, Data curation. **Krishna Prasad Sharma:** Validation, Methodology, Investigation, Formal analysis, Data curation. **In Hong Yang:** Writing – review & editing, Writing – original draft, Methodology, Investigation, Formal analysis, Data curation, Conceptualization. **Changho Yu:** Writing – review & editing, Writing – original draft, Supervision, Methodology, Investigation, Funding acquisition, Formal analysis, Data curation, Conceptualization.

## Declaration of competing interest

The authors declare that they have no known competing financial interests or personal relationships that could have appeared to influence the work reported in this paper.

## Acknowledgements

This work was supported by the National Research Foundation of Korea (NRF) grant, funded by the government of Korea (MSIT) (Project No. 2022R1A2C1093320), Technology Innovation Program (RS-2024-00434908, Development of a wearable light irradiation device for active drug release and wound treatment using stretchable light-emitting devices) funded by the Ministry of Trade Industry & Energy (MOTIE, Korea), and we are grateful to the Center for University-Wide Research Facilities (CURF) at Jeonbuk National University for their instrumental assistance.

## Data availability

Data will be made available on request.

## References

[1] E. Verdú, D. Ceballos, J.J. Vilches, X. Navarro, Influence of aging on peripheral nerve function and regeneration, J. Peripher. Nerv. Syst. 5 (4) (2000) 191–208.
[2] M.C. Dewan, A. Rattani, S. Gupta, R.E. Baticulon, Y.C. Hung, M. Punchak, A. Agrawal, A.O. Adeleye, M.G. Shrime, A.M. Rubiano, J.V. Rosenfeld, K.B. Park, Estimating the global incidence of traumatic brain injury, J. Neurosurg. 130 (4) (2018) 1080–1097.
[3] X. Zhang, M. Guo, Q. Guo, N. Liu, Y. Wang, T. Wu, Modulating axonal growth and neural stem cell migration with the use of uniaxially aligned nanofiber yarns welded with NGF-loaded microparticles, Mater. Today Adv. 17 (2023) 100343.
[4] J. Wu, H. Guo, L. Chen, Y. Wang, L. Sun, Biomaterials for peripheral nerve injury repair, J. Biomater. Tissue Eng. 13 (11) (2023) 1027–1045.
[5] B.E. Fornasari, G. Carta, G. Gambarotta, S. Raimondo, Natural-based biomaterials for peripheral nerve injury repair, Front. Bioeng. Biotechnol. 8 (2020).
[6] M.E. Harley-Troxell, R. Steiner, R.C. Advincula, D.E. Anderson, M. Dhar, Interactions of cells and biomaterials for nerve tissue engineering: polymers and fabrication, Polymers 15 (18) (2023) 3685.
[7] T.L. Rapp, C.A. DeForest, Tricolor visible wavelength-selective photodegradable hydrogel biomaterials, Nat. Commun. 14 (1) (2023) 5250.
[8] F. Tao, Y. Cheng, X. Shi, H. Zheng, Y. Du, W. Xiang, H. Deng, Applications of chitin and chitosan nanofibers in bone regenerative engineering, Carbohydr. Polym. 230 (2020) 115658.
[9] M. Kalogeropoulou, P.J. Díaz-Payno, M.J. Mirzaali, G.J.V.M. van Osch, L.E. Fratila-Apachitei, A.A. Zadpoor, 4D printed shape-shifting biomaterials for tissue engineering and regenerative medicine applications, Biofabrication 16 (2) (2024) 022002.
[10] I.S. Raja, S.H. Lee, M.S. Kang, S.-H. Hyon, A.R. Selvaraj, K. Prabakar, D.-W. Han, The predominant factor influencing cellular behavior on electrospun nanofibrous scaffolds: wettability or surface morphology? Mater. Des. 216 (2022) 110580.
[11] N. Haeri Moghaddam, S. Hashamdar, M.R. Hamblin, F. Ramezani, Effects of electrospun nanofibers on motor function recovery after spinal cord injury: a systematic review and Meta-analysis, World Neurosurg. 181 (2024) 96–106.
[12] Y.-S. Lee, T. Livingston Arinzeh, Electrospun Nanofibrous materials for neural tissue engineering, Polymers (2011) 413–426.
[13] D. Lee, H.Q. Tran, A.T. Dudley, K. Yang, Z. Yan, J. Xie, Advancing nerve regeneration: peripheral nerve injury (PNI) chip empowering high-speed biomaterial and drug screening, Chem. Eng. J. 486 (2024) 150210.
[14] Y. Dai, T. Lu, L. Li, F. Zhang, H. Xu, H. Li, W. Wang, M. Shao, F. Lyu, Electrospun composite PLLA-PPSB nanofiber nerve conduits for peripheral nerve defects repair and regeneration, Adv. Healthcare Mater. 13 (2024) 2303539.
[15] H.M. Pauly, D.J. Kelly, K.C. Popat, N.A. Trujillo, N.J. Dunne, H.O. McCarthy, T. L. Haut Donahue, Mechanical properties and cellular response of novel electrospun nanofibers for ligament tissue engineering: effects of orientation and geometry, J. Mech. Behav. Biomed. Mater. 61 (2016) 258–270.
[16] M. Moffa, A. Polini, A.G. Sciancalepore, L. Persano, E. Mele, L.G. Passione, G. Potente, D. Pisignano, Microvascular endothelial cell spreading and proliferation on nanofibrous scaffolds by polymer blends with enhanced wettability, Soft Matter 9 (23) (2013) 5529–5539.
[17] E. Zendedel, M. Javdani, S. Ebrahimi-Barough, J. Ai, M.R. Jaafari, S.A. Mirzaei, M. Soleimannejad, V.R. Askari, S. Asadpour, Development of small-diameter vascular grafts using PCL/PLA/gelatin/PVA/hyaluronic acid nanofibers containing VEGF/enoxaparin, J. Drug Delivery Sci. Technol. 101 (2024) 106171.
[18] S. Wu, K. Li, W. Shi, J. Cai, Chitosan/polyvinylpyrrolidone/polyvinyl alcohol/carbon nanotubes dual layers nanofibrous membrane constructed by electrospinning-electrospray for water purification, Carbohydr. Polym. 294 (2022) 119756.
[19] Q. Meng, Y. Li, Q. Wang, Y. Wang, K. Li, S. Chen, P. Ling, S. Wu, Recent advances of electrospun nanofiber-enhanced hydrogel composite scaffolds in tissue engineering, J. Manuf. Process. 123 (2024) 112–127.
[20] H. Rostamabadi, E. Assadpour, H.S. Tabarestani, S.R. Falsafi, S.M. Jafari, Electrospinning approach for nanoencapsulation of bioactive compounds; recent advances and innovations, Trends Food Sci. Technol. 100 (2020) 190–209.
[21] F. Zha, W. Chen, G. Lv, C. Wu, L. Hao, L. Meng, L. Zhang, D. Yu, Effects of surface condition of conductive electrospun nanofiber mats on cell behavior for nerve tissue engineering, Mater. Sci. Eng. C 120 (2021) 111795.
[22] K. Kim, M. Yu, X. Zong, J. Chiu, D. Fang, Y.-S. Seo, B.S. Hsiao, B. Chu, M. Hadjiargyrou, Control of degradation rate and hydrophilicity in electrospun non-woven poly(d,l-lactide) nanofiber scaffolds for biomedical applications, Biomaterials 24 (27) (2003) 4977–4985.
[23] Z. Mohammadalizadeh, E. Bahremandi-Toloue, S. Karbasi, Recent advances in modification strategies of pre- and post-electrospinning of nanofiber scaffolds in tissue engineering, React. Funct. Polym. 172 (2022) 105202.
[24] S. Wu, W. Shi, K. Li, J. Cai, C. Xu, L. Gao, J. Lu, F. Ding, Chitosan-based hollow nanofiber membranes with polyvinylpyrrolidone and polyvinyl alcohol for efficient removal and filtration of organic dyes and heavy metals, Int. J. Biol. Macromol. 239 (2023) 124264.
[25] P. Chen, P. Bergman, O. Blennow, L. Hansson, S. Mielke, P. Nowak, G. Söderdahl, A. Österborg, C.I.E. Smith, J. Vesterbacka, D. Wullimann, A. Cuapio, M. Akber, G. Bogdanovic, S. Muschiol, M. Åberg, K. Loré, M. Sällberg Chen, M. Buggert, P. Ljungman, S. Aleman, H.-G. Ljunggren, Real-world assessment of immunogenicity in immunocompromised individuals following SARS-CoV-2 mRNA vaccination: a one-year follow-up of the prospective clinical trial COVAXID, eBioMedicine 94 (2023) 104700.
[26] R. Sridhar, R. Lakshminarayanan, K. Madhaiyan, V.A. Barathi, K.H.C. Lim, S. Ramakrishna, Electrosprayed nanoparticles and electrospun nanofibers based on

natural materials: applications in tissue regeneration, drug delivery and pharmaceuticals, Chem. Soc. Rev. 44 (3) (2015) 790–814.
[27] A.P. Tiwari, B. Albin, K. Qubbaj, P. Adhikari, I.H. Yang, Phytic acid maintains peripheral neuron integrity and enhances survivability against platinum-induced degeneration via reducing reactive oxygen species and enhancing mitochondrial membrane potential, ACS Chem. Neurosci. 15 (6) (2024) 1157–1168.
[28] P.C. Scherer, Y. Ding, Z. Liu, J. Xu, H. Mao, J.C. Barrow, N. Wei, N. Zheng, S. H. Snyder, F. Rao, Inositol hexakisphosphate (IP6) generated by IP5K mediates cullin-COP9 signalosome interactions and CRL function, Proc. Natl. Acad. Sci. 113 (13) (2016) 3503–3508.
[29] Y. Chen, W. Yuan, Q. Xu, M.B. Reddy, Neuroprotection of phytic acid in Parkinson's and Alzheimer's disease, J. Funct. Foods 110 (2023) 105856.
[30] L.E. Nita, A.P. Chiriac, A. Ghilan, A.G. Rusu, N. Tudorachi, D. Timpu, Alginate enriched with phytic acid for hydrogels preparation, Int. J. Biol. Macromol. 181 (2021) 561–571.
[31] G.P. Awasthi, V.K. Kaliannagounder, J. Park, B. Maharjan, M. Shin, C. Yu, C. H. Park, C.S. Kim, Assembly of porous graphitic carbon nitride nanosheets into electrospun polycaprolactone nanofibers for bone tissue engineering, Colloids Surf. A Physicochem. Eng. Asp. 622 (2021) 126584.
[32] D. Verma, M. Okhawilai, N. Senthilkumar, N. Thirumalaivasan, A. Incharoensakdi, H. Uyama, Polyhydroxybutyrate/poly(ε-caprolactone)-based electrospun membranes loaded with amoxicillin-potassium clavulanate halloysite nanotubes for biomedical applications, Polym. Int. 74 (1) (2025) 54–65.
[33] G.P. Awasthi, V.K. Kaliannagounder, B. Maharjan, J.Y. Lee, C.H. Park, C.S. Kim, Albumin-induced exfoliation of molybdenum disulfide nanosheets incorporated polycaprolactone/zein composite nanofibers for bone tissue regeneration, Mater. Sci. Eng. C 116 (2020) 111162.
[34] N. Liao, A.R. Unnithan, M.K. Joshi, A.P. Tiwari, S.T. Hong, C.-H. Park, C.S. Kim, Electrospun bioactive poly (ε-caprolactone)–cellulose acetate–dextran antibacterial composite mats for wound dressing applications, Colloids Surf. A Physicochem. Eng. Asp. 469 (2015) 194–201.
[35] V. Rahimkhoei, M. Padervand, M. Hedayat, F. Seidi, E.A. Dawi, A. Akbari, Biomedical applications of electrospun polycaprolactone-based carbohydrate polymers: a review, Int. J. Biol. Macromol. 253 (2023) 126642.
[36] Y.-Y. Gao, C. Deng, Y.-Y. Du, S.-C. Huang, Y.-Z. Wang, A novel bio-based flame retardant for polypropylene from phytic acid, Polym. Degrad. Stab. 161 (2019) 298–308.
[37] Z. Tashi, M. Zare, N. Parvin, Application of phytic-acid as an in-situ crosslinking agent in electrospun gelatin-based scaffolds for skin tissue engineering, Mater. Lett. 264 (2020) 127275.
[38] M. Azizi, M. Azimzadeh, M. Afzali, M. Alafzadeh, S. Mirhosseini, Characterization and optimization of using *calendula officinalis* extract in fabrication of polycaprolactone-gelatin electrospun nanofibers for wound dressing applications 6, 2018, pp. 31–38.
[39] F. Kouhestani, M. Torangi, A. Motavalizadehkakhky, R. Karazhyan, R. Zhiani, Enhancement strategy of polyethersulfone (PES) membrane by introducing pluronic F127/graphene oxide and phytic acid/graphene oxide blended additives: preparation, characterization and wastewater filtration assessment, Desalin. Water Treat. 171 (2019) 44–56.
[40] M. Sharahi, A. Hivechi, H. Bahrami, N. Hemmatinejad, P. Milan, Co-electrospinning of lignocellulosic nanoparticles synthesized from walnut shells with poly(caprolactone) and gelatin for tissue engineering applications, Cellulose 28 (2021).
[41] Y. Hong, H. Zhao, C. Pu, Q. Zhan, Q. Sheng, M. Lan, Hydrophilic Phytic Acid-Coated Magnetic Graphene for Titanium(IV) Immobilization as a Novel Hydrophilic Interaction Liquid Chromatography–Immobilized Metal Affinity Chromatography Platform for Glyco- and Phosphopeptide Enrichment with Controllable Selectivity, Anal. Chem. 90 (18) (2018) 11008–11015.
[42] S.A. Lee, M.R. Bedford, Inositol - an effective growth promotor? Worlds Poult. Sci. J. 72 (4) (2016) 743–760.
[43] S. Sell, C. Barnes, M. Smith, M. McClure, P. Madurantakam, J. Grant, M. Mcmanus, G. Bowlin, Extracellular matrix regenerated: tissue engineering via electrospun biomimetic nanofibers, Polym. Int. 56 (11) (2007) 1349–1360.
[44] A.P. Tiwari, M.K. Joshi, J.I. Kim, A.R. Unnithan, J. Lee, C.H. Park, C.S. Kim, Bimodal fibrous structures for tissue engineering: fabrication, characterization and in vitro biocompatibility, J. Colloid Interface Sci. 476 (2016) 29–34.
[45] P. Chandra Lohani, A. Prasad Tiwari, A. Muthurasu, I. Pathak, M. Babu Poudel, K. Chhetri, B. Dahal, D. Acharya, T. Hoon Ko, H. Yong Kim, Phytic acid empowered two nanos "Polypyrrole tunnels and transition metal-(oxy)hydroxide sheets" in a single platform for unmitigated redox water splitting, Chem. Eng. J. 463 (2023) 142280.
[46] A. Ghilan, M. Bercea, A.G. Rusu, N. Simionescu, A.M. Serban, A. Bargan, L.E. Nita, A.P. Chiriac, Self-healing injectable hydrogels incorporating hyaluronic acid and phytic acid: rheological insights and implications for regenerative medicine, Int. J. Biol. Macromol. 279 (2024) 135056.
[47] S.E. Kim, A.P. Tiwari, Three dimensional polycaprolactone/cellulose scaffold containing calcium-based particles: a new platform for bone regeneration, Carbohydr. Polym. 250 (2020) 116880.